quantum band model (*55*) to 50 K and used it to obtain a *g* factor for the *Q*-branch region and an upper limit to the CH_3OH production rate.
54. R. H. Hunt *et al.*, *J. Mol. Spectrosc.* **149**, 252 (1991).
55. D. C. Reuter, *Astrophys. J.* **386**, 330 (1992).
56. Li-H. Xu *et al.*, *J. Mol. Spectrosc.* **185**, 158 (1997).
57. We tailored our ethane fluorescence model (*45*) to 50 K rotational temperature.
58. T. L. Farnham *et al. Science* **292**, 1348 (2001).
59. H. A. Weaver *et al. Science* **292**, 1329 (2001).
60. D. Bockelée -Morvan *et al.*, *Science* **292**, 1339 (2001).
61. The water production rate reported by (*59*) may need downward revision, if OH electronic prompt emission is significant (*62*). HST fluxes show a continual decrease from July 6.74 to July 6.87, so the peak production apparently occurred before July 6.74 (*59*).
62. S. A. Budzien, P. D. Feldman, *Icarus* **90**, 308 (1991).
63. J. T. T. Mäkinen *et al.*, *Science* **292**, 1326 (2001).
64. P. Eberhardt *et al.*, *Space Sci. Rev.* **90**, 45 (1999).
65. The CO mixing ratio reported by (*25*) is being revised upward because of optical depth effects (*27*) and improvements in our data processing techniques (*47*).
66. Our upper limit obtained for C_2H_2 shows that it is less abundant in C/LINEAR than in the four comparison comets; for example, in Lee $C_2H_2/H_2O = 0.27 \pm 0.03$ and in Hale-Bopp $C_2H_2/H_2O = 0.31 \pm 0.1\%$ (*10*).
67. G. Notesco, A. Bar-nun, *Icarus* **122**, 118 (1996).
68. G. Notesco *et al.*, *Icarus* **125**, 471 (1997).
69. K. R. Lang, *Astrophysical Quantities* (Springer, Berlin, 1980), p. 162.
70. Bockelée-Morvan *et al.* (*60*) assumed the mixing ratio (HCN/H_2O) to be 0.1% in C/LINEAR. Radio measurements generally show cometary $HCN/H_2O \sim 0.1\%$ (*15*), but IR measurements show differences among comets. For example, on 13.8 July, HCN in C/LINEAR ($\sim 0.10 \pm 0.03$) was less than that in comets Lee ($0.23 \pm 0.02\%$) and Hale-Bopp ($0.40 \pm 0.05\%$) (*10*, *29*). Differences between radio and IR measurements are not understood at present. The CN/OH ratio is also low in C/LINEAR (*58*), as compared with comets Halley, Hyakutake, and Hale-Bopp. However, NH/OH is normal (*58*), as are our NH_2/OH line intensities (Fig. 2D).
71. P. Eberhardt *et al.*, *Astron. Astrophys.* **288**, 315 (1994).
72. D. Despois *et al.*, *Earth Moon Planets* **79**, 103 (1999).
73. J. Hatchell *et al.*, *Astrophys. J.* **338**, 713 (1998).
74. S. B. Charnley *et al.*, *Astrophys. J.* **399**, L71 (1992).
75. A. Drouart *et al.*, *Icarus* **140**, 129 (1999).
76. O. Mousis *et al.*, *Icarus* **148**, 513 (2000).
77. J. Nuth *et al.*, *Nature* **406**, 275 (2000).
78. D. Bockelée-Morvan *et al.*, *Bull. Am. Astron. Soc.* **32**, 1081 (2000).
79. Recent models of gas phase chemistry in the protoplanetary disk have reproduced the deuterium enrichment seen in HCN and H_2O in Hale-Bopp (*80*).
80. Y. Aikawa, E. Herbst, *Astrophys. J.* **526**, 314 (1999).
81. We use the term "Jovian-class" to mean a comet that formed in the Jupiter-Saturn nebular region. This should not be confused with the term "Jupiter-family" comet. The Jupiter-family comets are a dynamical grouping with Tisserand invariant $2 < T_j < 3$; they formed over a much wider range of heliocentric distance (from the Kuiper belt inward) and only later entered their present orbits.
82. A. Delsemme, *Planet. Space Sci.* **47**, 125 (1998).
83. A. Delsemme, *Icarus* **146**, 313 (2000).
84. Supported by the NASA Planetary Astronomy Program (grants RTOP 344-32-30-07 to M.J.M. and NAG5-7905 to M.A.D.), by the NASA Planetary Atmospheres Program (grant NAG5-7753 to N.D.R.), and by NSF (grant AST-9619461 to K.M.S.). The NASA IRTF is operated by the University of Hawaii under contract to NASA. The Keck Observatory was made possible by the generous financial support of the W. M. Keck Foundation; it is operated as a scientific partnership among the California Institute of Technology, the University of California, and NASA. We thank the staff of IRTF and Keck for their expert assistance and H. Levison for valuable discussions. M.J.M. thanks S. T. Mumma and S. E. Selonick, without whose support this research would not have been possible.

10 January 2001; accepted 2 April 2001

COMET C/LINEAR

Outgassing Behavior and Composition of Comet C/1999 S4 (LINEAR) During Its Disruption

Dominique Bockelée-Morvan,[1] Nicolas Biver,[1] Raphaël Moreno,[2] Pierre Colom,[1] Jacques Crovisier,[1] Éric Gérard,[1] Florence Henry,[1] Dariusz C. Lis,[3] Henry Matthews,[4] H. A. Weaver,[5] Maria Womack,[6] Michel C. Festou[7]

The gas activity of comet C/1999 S4 (LINEAR) was monitored at radio wavelengths during its disruption. A runaway fragmentation of the nucleus may have begun around 18 July 2000 and proceeded until 23 July. The mass in small icy debris (≤30-centimeter radius) was comparable to the mass in the large fragments seen in optical images. The mass budget after breakup suggests a small nucleus (~100- to 300-meter radius) that had been losing debris for weeks. The HNC, H_2CO, H_2S, and CS abundances relative to H_2O measured during breakup are consistent with those obtained in other comets. However, a deficiency in CH_3OH and CO is observed.

Cometary nuclei are porous bodies containing ices and refractory material. It is not uncommon for cometary nuclei to split into several fragments (*1, 2*), which demonstrates their fragile nature. In addition, a number of comets have been observed to disappear catastrophically (*3*), which suggests their disintegration into small debris being stripped of their ices on short time scales. Owing to the unpredictable nature of such events, data on the evolution of the gaseous activity of a cometary nucleus undergoing disruption are sparse. So far, gas monitoring observations of a fragmenting comet were only obtained for 73P/Schwassmann-Wachmann 3 (*4*).

Comet C/LINEAR's close approach to Earth at 0.374 astronomical units (AU; 1 AU = 1.496×10^{11} m is the average Earth-Sun distance), just a few days before perihelion on 26 July 2000, when the comet was 0.765 AU from the Sun, together with favorable brightness predictions, made this comet a suitable target for spectroscopic observations at radio wavelengths. This spectral range allows the study of many volatile molecular species released by the nucleus as it approaches the Sun (*5–9*). Radio observations of C/LINEAR were planned to expand our data sample used for comparative studies of cometary composition. Serendipitously, they provided unprecedented data on the outgassing behavior of a nucleus undergoing almost complete disruption.

The observations were made with five different radio telescopes. OH 18-cm observations were scheduled from 6 July to 3 August 2000 at the Nançay radio telescope, upgraded with a new focus system (*10*). These observations were aimed at providing the production rate of water, which is the source of the OH radical and the most abundant constituent of cometary ices. Observations in the millimeter and submillimeter ranges were performed with the National Radio Astronomy Observatory (NRAO) 12-m Kitt Peak telescope, the Caltech Submillimeter Observatory (CSO, 10.4 m), the James Clerk Maxwell Telescope (JCMT, 15 m), and the Institut de Radio Astronomie Millimétrique (IRAM) 30-m telescope. Data were acquired in early January 2000, when comet C/LINEAR was still at the distance $r_h = 3.2$ AU from the Sun, on 17 to 20 June 2000 ($r_h = 1.0$ AU), 1 July ($r_h = 0.9$ AU), and almost daily around perihelion from 18 July to 3 August ($r_h \sim 0.77$ AU). Seven molecular species were searched for (HCN, HNC, CO, H_2CO, CH_3OH, H_2S, and CS), some of them through several rotational transitions (Table 1). All species, except CO and CH_3OH, were detected (Figs. 1 and 2). In contrast to other species, which were observed only on selected dates, HCN was continuously monitored during the scheduled observing periods (Table 1).

The observed line intensities were converted into gas production rates with standard techniques (*7, 11–13*). In a normally behaved comet, one would expect the outgassing rates to follow a rather smooth r_h^{-n} law, with n ranging from 2 to 4. However, observations of the HCN, H_2O (*14*), OH (*15, 16*) (Fig. 3),

[1]Observatoire de Paris-Meudon, F-92195, Meudon, France. [2]Institut de Radioastronomie Millimétrique, 300 rue de la Piscine, Domaine Universitaire, F-38406, St. Martin d'Hères Cedex, France. [3]Department of Physics, California Institute of Technology, MS 320-47, Pasadena, CA 91125, USA. [4]Joint Astronomy Centre, 660 North A'ohoku Place, Hilo, HI 96720, USA. [5]Johns Hopkins University, 3400 North Charles Street, Baltimore, MD 21218–2686, USA. [6]St. Cloud State University, 720 Fourth Avenue S, MS 324, St. Cloud, MN 56301–4498, USA. [7]Observatoire Midi-Pyrénées, 14 avenue Edouard Belin, F-31400, Toulouse, France.

and H Lyman-α emissions (*17*) collected in June and July 2000 show that the gaseous activity of C/LINEAR was different. HCN production rates were converted into H_2O production rates assuming Q[HCN]/Q[H_2O] = 0.001, the value commonly derived from radio range data and also measured in this comet in July 2000 (*14, 15*) (Fig. 3). Several possible outbursts of activity are noticeable in the water production rate curve (e.g., 10 to 12 June, 6 July) (*15–17*). A progressive 10-fold increase in activity was observed between 18.6 and 23.9 July, followed by a rapid decrease over the next 3 days (24 to 26 July) down to a level ~eight times below the outgassing rate recorded on 18 July. The total visual magnitude, which is sensitive to the dust and gas production rates, showed a similar trend, although of much weaker amplitude (Fig. 3). During the same period, the dust coma displayed structural changes, suggesting that this peculiar outgassing behavior was linked to the disruption of the nucleus. The coma displayed on 23.9 July the typical teardrop shape with a strong central condensation, but shortly thereafter the coma became more and more elongated, while the central condensation decreased rapidly in brightness and was no longer visible on 27.9 July (*18*). Images taken with the Hubble Space Telescope (HST) and the Very Large Telescope (VLT) on 5 and 6 August, respectively, revealed multiple (~16) active fragments near the expected position of the nucleus of C/LINEAR (*16*).

When a cometary nucleus breaks up into debris, a larger surface area of icy material is exposed to solar radiation, and this results in a higher production rate of volatiles in the coma. The subsequent evolution of the comet's activity depends on the size distribution of the debris. Small pieces have a large cross section relative to their mass and contribute predominantly to the outgassing surge. Small objects also disappear fast because their volatile content is soon exhausted. If the size distribution of the comet debris is dominated by small particles, the outgassing surge can be brief and will be followed by a rapid decrease of gas production down to a level lower than the value before fragmentation. In contrast, sustained activity, at a level greater than that before breakup, may be expected when large fragments dominate. The lifetime of icy fragments of radius a (cm) exposed to solar illumination can be estimated from τ_d [day] = 0.14 × a at r_h = 0.77 AU, assuming a bulk density ρ = 0.5 g cm^{-3} and an ice-to-dust mass ratio κ = 1 (*19*). With the use of dust terminal velocities derived from the theory of dust acceleration by gas-dust momentum transfer (*20, 21*), the distance traveled by icy grains before complete evaporation is estimated to be L_d [km] = 250 × $a^{0.5}$ Q[H_2O]$^{0.5}$ for a nucleus whose radius is 500 m, where Q[H_2O] is the water production rate in units of 10^{29} molecules s^{-1}. Travel distances for grains with radii smaller than a few tens of centimeters are small compared with the radius of the field of view used during our radio observations, so that the nuclear source density distribution assumed for the production rate determinations (*13*) should be valid if these grains are the dominant source of gas (*22*). Large fragments, possibly of 1 m size or larger, nonuniformly illuminated by the Sun, should be accelerated by nongravitational forces and might escape the central part of the coma we observed. Consequently, their contribution to the gas production would be underestimated by our calculations.

The progressive increase in activity from

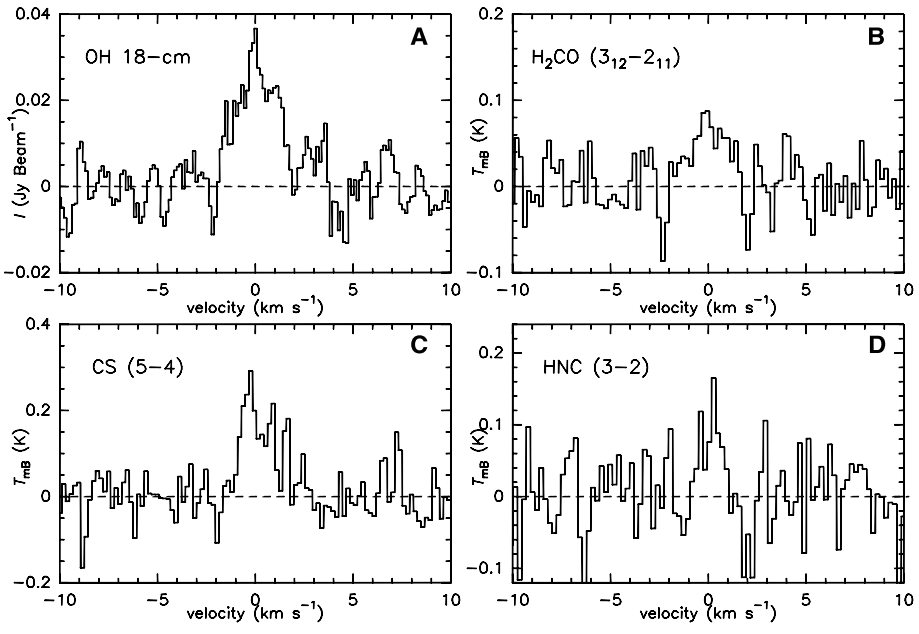

Fig. 1. A selection of radio spectra of comet C/1999 S4 (LINEAR). (**A**) Average of the 1667- and 1665-MHz lines of the OH radical (scaled to 1667 MHz) observed from 6 to 9 July 2000 at the Nançay radio telescope. (**B**) H_2CO 3_{12}–2_{11} line at 225.7 GHz observed at the IRAM 30-m telescope on 20 to 21 July 2000. (**C**) CS J(5–4) line at 244.9 GHz observed at the IRAM 30-m telescope on 20 to 21 July 2000. (**D**) HNC J(3–2) line at 272.0 GHz observed at the IRAM 30-m telescope on 24 July 2000. The horizontal axis is the radial velocity with respect to the comet rest velocity, projected along the line of sight. The vertical axis shows the main beam brightness temperature (T_{mB}), except for the OH line, for which the intensity is given in units of janskys beam^{-1} (Jy; 1 Jy = 10^{-26} W m^{-2} Hz^{-1}).

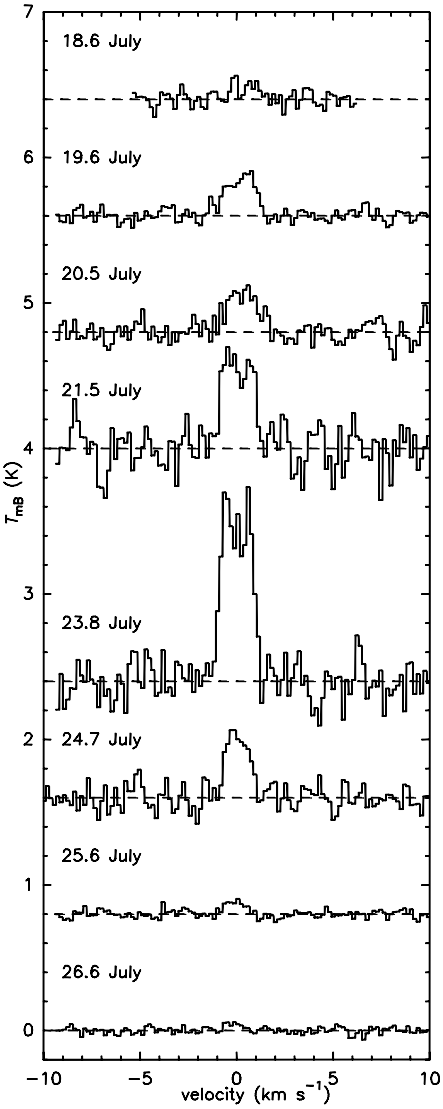

Fig. 2. The HCN J(3–2) line at 265.9 GHz observed in comet C/1999 S4 (LINEAR) from 18 to 26 July 2000 at the IRAM 30-m telescope. The vertical and horizontal axes are similar to those of Fig. 1. Spectra are scaled identically, but they have been shifted vertically by observation dates. The dashed lines show their zero level.

18 to 23 July suggests that the nucleus of comet C/LINEAR underwent successive steps of fragmentation. The area of exposed icy material increased by a factor of ~10 in 5 days (*23*). If the gas-to-dust mass production ratio is 1, the gaseous production during 18 to 23.9 July translates into a minimum mass loss of material $\delta m_{18\rightarrow23} = 1.1 \times 10^9$ kg (Table 2), which is the mass contained within a compact sphere having a radius of 81 m, assuming $\rho = 0.5$ g cm^{-3}.

The rapid decrease in gas production during 23.9 to 24.7 July suggests that the fragmentation phase ended shortly after 23.9 July UT. It also indicates that icy fragments of small sizes were then present in copious amounts. If one assumes that the fragmentation stopped around 23.9 July, the decrease of the HCN production rate between 24.7 and 27.8 July can be explained by sublimating grains of a single size $a \sim 20$ cm radius and lifetime ~2.8 days (*19*). A size distribution $a^{-3.5}$ on 23.9 July reproduces the observed decrease in HCN production, providing a maximum size allowed of $a_{max} = 30$ cm (*24*). The gas production measured after 23.9 July corresponds to a mass loss in dust and ices $\delta m_{23\rightarrow27} = 4.4 \times 10^8$ kg for $\kappa = 1$, mainly released by decimeter-sized icy chunks. A large mass of material could have been produced by icy grains of smaller sizes, if the size distribution after fragmentation was steeper than a^{-4}. The absence of strong surges in brightness in the visual light curve (Fig. 3), the mass in the dust tail on 2 August (~ 4×10^8 kg) (*16*), and the low mass losses measured from H Lyman-α observations (*17*) suggest that this was probably not the case. The mass in the dust tail, when compared with the gas mass loss rate (Table 2), is consistent with $\kappa \sim 1$.

Large nuclearlike fragments, such as those observed during the HST and VLT observations (*16*), apparently do not contribute substantially to the gas production measured after 24 July. Adopting an upper limit of $Q_{H_2O} < 10^{27}$ molecules s^{-1} derived from the HCN observations of 28.7 July, we estimate that the

Table 1. Log of selected observations. r_h and Δ are the heliocentric and geocentric distances, respectively. Temperature scale for the line areas is main beam brightness temperature. The diffraction limited beam diameter (in arc sec) scales approximately as 2400/ν, 4860/ν, 6000/ν, at the IRAM 30-m, JCMT 15-m, and NRAO 12-m telescopes, respectively, where ν is the frequency in GHz. The Nançay elliptical beam is 3.5 arc min in right ascension (RA) and 19 arc min in declination. Because of ephemeris errors, the beam is offset by ~3 to 6 arc sec in July, ~8 arc sec on 17 June, and ~3 arc sec on 19 to 20 June for millimeter observations. Beam offsets for the Nançay observations are 0.8 arc min and 2.7 arc min in RA, on 6 to 9 July and 13 to 19 July, respectively. The quoted uncertainties are 1σ values. Upper limits are 3σ values.

UT date (mm/dd.d)	$< r_h >$ (AU)	$< \Delta >$ (AU)	Line area (K km s^{-1})							OH (mJy km s^{-1})
			HCN	HNC(3–2)	CS(5–4)	H_2S ($1_{10}-1_{01}$)	H_2CO ($3_{12}-2_{11}$)	CH_3OH	CO	
JCMT 15 m			*J*(4–3) line						*J*(3–2) line	
06/17.8	1.06	1.46	0.07 ± 0.02							
06/19.7	1.03	1.39	0.17 ± 0.01						<0.03	
06/20.7	1.02	1.36	0.20 ± 0.03					<0.13*		
NRAO 12 m			*J*(1–0) line							
07/01.9	0.90	0.96	0.19 ± 0.04							
IRAM 30 m			*J*(3–2) line						*J*(2–1) line	
07/18.6	0.78	0.42	0.18 ± 0.03		<0.07			<0.06†	< 0.07	
07/19.6	0.78	0.40	0.50 ± 0.03					<0.08†	<0.04	
07/20.6	0.77	0.39	0.54 ± 0.05		0.15 ± 0.04‡		0.05 ± 0.02			
07/21.6	0.77	0.38	1.20 ± 0.09		0.37 ± 0.03	0.10 ± 0.03	0.14 ± 0.02			
07/23.8	0.77	0.38	2.19 ± 0.08					<0.26†	<0.13	
07/24.7	0.77	0.38	0.69 ± 0.05	0.13 ± 0.04		0.05 ± 0.02				
07/25.7	0.76	0.39	0.13 ± 0.02					<0.06†		
07/26.7	0.76	0.41	0.05 ± 0.01							
07/28.7	0.77	0.45	<0.04							
Nançay										18-cm lines¶
07/06–09	0.85	0.76								82 ± 10
07/13–19	0.79	0.48								−22 ± 8

*Sum of four lines at 338 GHz. †Sum of five lines at 157 GHz. ‡The CS(3–2) line is also detected and yields the same production rate. ¶From average 1667 and 1665 MHz lines, scaled to 1667 MHz.

Table 2. Mass budget. m_{18} is the nucleus mass needed to account for $Q_{H_2O} = 8 \times 10^{27}$ molecules s^{-1} on 18.6 July. $\delta m_{18\rightarrow23}$ and $\delta m_{23\rightarrow27}$ are the total masses lost during the 18.6 to 23.8 July and 23.8 to 27 July periods, respectively. m_{28} is the mass upper limit in 16 fragments of equal sizes derived from $Q_{H_2O} < 10^{27}$ molecules s^{-1} on 28.7 July. $\delta m_{18\rightarrow}$ is equal to $\delta m_{18\rightarrow23} + \delta m_{23\rightarrow27} + m_{28}$. $r(\delta m_{18\rightarrow})$ is the radius of the compact sphere with mass $\delta m_{18\rightarrow}$. The nucleus and fragments masses are computed with two thermal models (*20, 23*): Model 1 assumes perfect thermal contact between ice and grains at the surface (local isothermal approximation); model 2 assumes that the ice is thermally isolated from the grains (zero thermal conductivity approximation). Both models use the simplifying assumption of fast-rotating objects. Unless specified otherwise, discussion in the text is based on model 2.

Ice/dust ratio	Pure ice	κ = 1		κ = 1/10		κ = 1/10	
Density	ρ = 0.5	ρ = 0.5		ρ = 0.5		ρ = 0.1 g cm^{-3}	
Thermal model		1	2	1	2	1	2
m_{18} (kg)	6.1×10^{10}	6.1×10^{10}	1.7×10^{11}	6.1×10^{10}	2.2×10^{12}	1.2×10^{10}	4.5×10^{11}
$\delta m_{18\rightarrow23}$ (kg)	5.7×10^8	1.1×10^9	1.1×10^9	6.2×10^9	6.2×10^9	6.2×10^9	6.2×10^9
$\delta m_{23\rightarrow27}$ (kg)	2.2×10^8	4.4×10^8	4.4×10^8	2.4×10^9	2.4×10^9	2.4×10^9	2.4×10^9
m_{28} (kg)	6.7×10^8	6.7×10^8	1.9×10^9	6.7×10^8	2.5×10^{10}	1.3×10^8	5.0×10^9
$\delta m_{18\rightarrow}/m_{18}$	2.4%	3.6%	2.0%	15%	1.5%	71%	3.0%
$r(\delta m_{18\rightarrow})$ (m)	89	102	119	164	253	275	320

total area of sublimating icy material is less than 0.15 km^2 (*23*). If this icy area is distributed among 16 identical fragments, each with a density of 0.5 g cm^{-3} and an icy area fraction of 50% corresponding to $\kappa = 1$, the effective radius of each fragment would be ~40 m and the total mass in the system would be $\sim 2 \times 10^9$ kg (Table 2 with thermal model 2) (*23*). This limit for the total mass contained in large fragments is only a factor of four larger than the mass found in the ~30-cm debris that produced the observed gaseous production rate after 23.9 July and is comparable to the mass of gas and dust produced during 18 to 27 July. The other (ρ, κ) values tested provide the same qualitative result (Table 2). Therefore, we can conclude that the nucleus of C/LINEAR broke up, in large part, in a cloud of particulate debris. However, it is still possible that most of the mass of C/LINEAR was in inactive or low-activity fragments with ice-to-dust mass ratios much lower than that of the icy debris. The large fragment masses derived from their optical observations, if accurate, would favor this scenario (*16*).

The mass budget of volatiles, dust particles, and fragments released after 18 July, $\delta m_{18\rightarrow}$, is very small compared with the mass, m_{18}, contained in a compact sphere with the icy area of 1.2 km^2 that is needed to support the gaseous production rate measured on 18 July (Table 2). With our nominal parameters, $\rho = 0.5$ g cm^{-3} and $\kappa = 1$, and the thermal model 2, we find $\delta m_{18\rightarrow}/m_{18} < 2\%$ (Table 2). This ratio can be increased to almost unity, if one assumes much lower ρ and κ [e.g., $\rho = 0.1$ g cm^{-3} and $\kappa = 0.1$ in the extreme high thermal conductivity approximation of thermal model 1, which is unrealistic for such low (ρ, κ) values; Table 2], an assumption that implies a high porosity of the nucleus. A more likely explanation is that icy grains were already contributing to the gas production on 18 July. Because the mass budget is equivalent to a compact sphere of at most 100 to 300 m radius (Table 2), this suggests a small size for the nucleus of C/LINEAR and a comparatively large contribution of icy grains to the gas activity on 18 July. Evidence that cm-sized icy grains could be a major secondary source of water vapor was already found when comet C/1996 B2 (Hyakutake) was undergoing fragmentation (*25*). The still higher production rates in C/LINEAR measured before 18 July, the drop of activity after 13 July, and the many gas outbursts reported (Fig. 3) (*15–17*) suggest that the comet was continuously losing debris, at least several weeks before its total disruption.

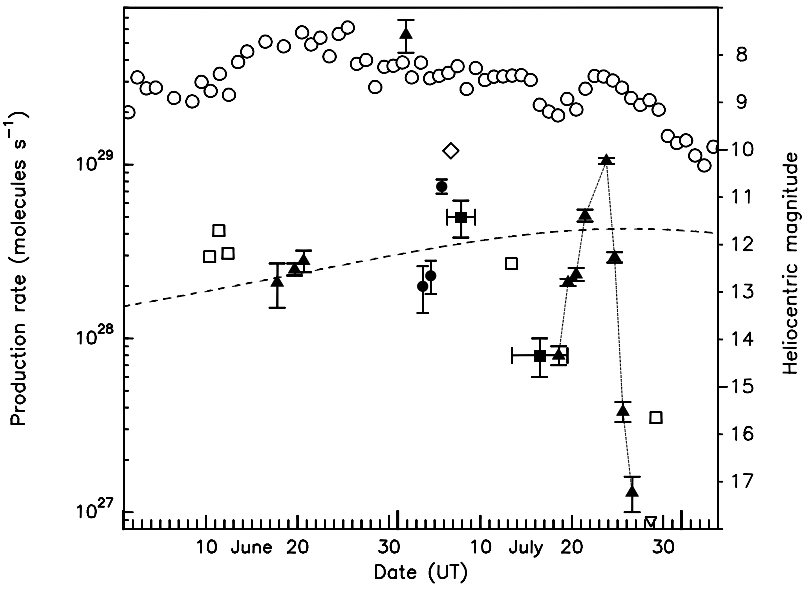

Fig. 3. Evolution of the H_2O production rate and heliocentric total visual magnitude of C/1999 S4 (LINEAR) during June to August 2000. H_2O production rates (▲) or upper limits (▽) derived from HCN observations adopting $Q[HCN]/Q[H_2O] = 10^{-3}$. H_2O production rates derived from OH observations: Nançay (■), ground-based UV (*15*) (□), and HST UV (*16*) (◇). H_2O observations: IR (●) (*14*). Heliocentric visual magnitudes, taken from (*30*), that have been daily averaged (○). The dashed curve is the r_h^{-2} variation expected from simple sublimation models of nuclear ices. The HCN data suggest that a huge outburst, not seen by (*17*), occurred on 1 July. Note that, in contrast to gas observations, the visual magnitude samples the whole coma made of dust particules of different ages. Consequently, the variations in visual magnitude are much smaller than the variations in gas production rate.

Table 3. Production rates Q relative to water. They were deduced from Q/Q[HCN], assuming $Q[HCN]/Q[H_2O] = 0.1\%$. For nondetections, 3σ upper limits are quoted, except for CH_3OH for which we give the 4σ upper limit. Indeed, a marginal signal at the 4σ level is observed.

Species	Date range	$Q/Q[H_2O]$
HCN	June 17.7 to July 26.7	Assumed 0.1%
CO	June 20.1	<8.4%
	July 23.8	<7.2%
CH_3OH	July 23.8	≤0.96%
H_2CO	July 20.6–21.6	0.56 ± 0.13%
CS	July 20.6–21.7	0.12 ± 0.02%
H_2S	July 21.4–24.7	0.34 ± 0.1%
HNC	July 24.7	0.017 ± 0.006%

The measured chemical abundances (Table 3) provide information on the composition of the ice in the nucleus at the time of fragmentation. This is in contrast to determinations made in previous comets, for which it could be argued that chemical differentiation in the upper layers of the nucleus might make the chemical abundances measured in the coma not fully representative of the bulk composition of the nucleus. All species, except HNC, were observed on at least two different days during the 18 to 25 July period (Table 1). Even though the HCN production rate varied substantially during this time, the abundances relative to HCN for the individual days are constant within the uncertainties. In other words, the relative abundances did not change during the breakup phase, indicating that the nucleus had a homogeneous composition.

HNC, H_2CO, H_2S, and CS production rates relative to water are in the range of those measured in other comets (*7, 9, 11, 26*). The upper limit obtained for the CO relative abundance demonstrates that comet C/LINEAR is CO-depleted when compared with comets Hale-Bopp and Hyakutake (*7, 9*). Emissions from CO were detected at ultraviolet (UV) (*16*) and infrared (IR) (*14*) wavelengths on 5 July, and the derived CO abundance is only ~1%. We did not securely detect CH_3OH and obtained an upper limit of ~1% on its relative abundance (Table 3), showing that C/LINEAR is also depleted in CH_3OH. The upper limit set by IR observations (0.2%) is even lower (*14*). Methanol abundances vary widely (1 to 8%) (*26, 27*) from comet to comet. Comet C/1996 Q1 (Tabur), which also underwent catastrophic disruption (*28, 29*), also belongs to the class of CH_3OH-depleted comets ($Q[CH_3OH]/Q[H_2O] < 1.4\%$) (*26*).

Cometary ices trace the molecular composition of the solar nebula in the giant planets' region where they formed, as well as the temperature environment that led to their condensation. Ices found in comet Hale-Bopp had many similarities with the ices present in

star-forming regions, suggesting that the outer parts of the solar nebula inherited, to a large extent, the composition of the protosolar cloud (*9*). The CO depletion inferred in C/LINEAR ices might reflect their formation at higher temperatures than for Hale-Bopp, that is, closer to the Sun (*14*). However, given the small size of C/LINEAR nucleus and its high level of activity at $r_h = 4$ AU, which is better explained by CO sublimation (*5, 6*), a depletion of the CO reservoir well before perihelion cannot be excluded. The CH_3OH depletion, compared with normal abundances in species with similar volatilities (HCN), is difficult to explain by these two mechanisms.

References and Notes

1. Z. Sekanina, in *Comets*, L. L. Wilkening, Ed. (Univ. of Arizona Press, Tucson, AZ, 1982), pp. 251–287.
2. J. Chen, D. Jewitt, *Icarus* **108**, 265 (1994).
3. Z. Sekanina, *Icarus* **58**, 81 (1984).
4. J. Crovisier *et al*., *Astron. Astrophys.* **310**, L17 (1996).
5. N. Biver *et al*., *Science* **275**, 1915 (1997).
6. N. Biver *et al*., *Earth Moon Planets* **78**, 5 (1999).
7. N. Biver *et al*., *Astron. J.* **118**, 1850 (1999).
8. P. Colom *et al*., *Earth Moon Planets* **78**, 37 (1999).
9. D. Bockelée-Morvan *et al*., *Astron. Astrophys.* **353**, 1101 (2000).
10. W. van Driel, J. Pezzani, E. Gérard, in *High Sensitivity Radio Astronomy*, N. Jackson, R. J. Davis, Eds (Cambridge Univ. Press, Cambridge, 1996), pp. 229–232.
11. N. Biver *et al*., *Astron. J.* **120**, 1554 (2000).
12. D. Bockelée-Morvan *et al*., *Planet. Space Science* **42**, 193 (1994).
13. We made the assumption of steady-state isotropic outflow. OH 18-cm lines were analyzed following (*12*) with an H_2O outflow velocity assumed to be 1.0 km s^{-1}. For the species observed in the millimeter range, we used a nuclear source distribution for the local density, except for CS and H_2CO, which were assumed to come from a distributed source with parent lifetimes of $340 \times r_h^2$ s and $8000 \times r_h^2$ s, respectively (*7, 11*). The outflow velocity was estimated from the widths of the HCN lines to be 0.65, 0.7, 0.9 to 0.95, 0.75, and 0.60 km s^{-1} for the 17 to 20 June, 1 July, 18 to 23 July, 24.7 July, and 25.7 to 28.7 July periods, respectively. Rotational lines observed in the millimetric and submillimetric domains were analyzed with the excitation model of (*7, 11*), adopting a gas kinetic temperature of 50 K for June and of 70 K for July consistent with temperature determinations in low-activity comets. Beam offsets were taken into account in the calculations.
14. M. J. Mumma *et al*., *Science* **292**, 1334 (2001).
15. T. L. Farnham *et al*., *Science* **292**, 1348 (2001).
16. H. A. Weaver *et al*., *Science* **292**, 1329 (2001).
17. J. T. T. Mäkinen, J.-L. Bertaux, M. R. Combi, E. Quémarais, *Science* **292**, 1326 (2001).
18. M. Kidger *et al*., *IAU Circ. 7467* (2000).
19. The lifetime of spherical icy grains has been calculated from $\tau_d = \rho a (1 + \kappa^{-1})^{-1} r_h^2 / m_{H_2O} Z_{H_2O}$, where ρ is the grain density, a is the grain radius, κ is the gas-to-dust mass ratio, m_{H_2O} is the H_2O molecular mass, and Z_{H_2O} is the H_2O sublimation rate per unit surface at $r_h = 1$ AU. We use $Z_{H_2O} = 4 \times 10^{17}$ molecules cm^{-2} s^{-1}, corresponding to a fast rotator with geometrical albedo of 0.04. We assume $\rho = 0.5$ g cm^{-3} and $\kappa = 1$. At $r_h = 0.77$ AU, $\tau_d/a = 0.14$ day cm^{-1}.
20. J. F. Crifo, A. V. Rodionov, *Icarus* **127**, 319 (1997).
21. The terminal velocity of spherical grains accelerated by gas-dust momentum transfer is $V_d = 1.4\, a^{-0.5} V_{\infty,exp} \, (Q[H_2O] m_{H_2O} / 4\pi R_n \rho V_{0,exp})^{0.5}$ for a water-dominated coma. $V_{0,exp}$ and $V_{\infty,exp}$ are, respectively, the gas initial and terminal velocities, $Q[H_2O]$ and m_{H_2O} are defined in (*19*), ρ is the grain density, and R_n is the nucleus radius (*20*). Calculations of $L_d = V_d \times \tau_d$ assume $V_{0,exp} = 0.3$ km s^{-1}, $V_{\infty,exp} = 0.8$ km s^{-1} and $\rho = 0.5$ g cm^{-3}.
22. From the line intensities obtained at offset positions 10 to 15 arc sec from the nucleus on 18 to 25 July, we do not see any evidence for an extended distribution of HCN gas. Substantial departure from a nuclear source distribution is only observed on 19.6 July and is likely due to short-term variations.
23. The sublimating icy area S_{icy} is related to the H_2O production rate through $Q[H_2O] = S_{icy} Z_{H_2O}$, where Z_{H_2O} is the H_2O sublimation rate per unit surface at r_h. In the case of thermally isolated ice (model 2 in Table 2), $Z_{H_2O} = F_{sol}(1 - A)/4L_{H_2O}$, where F_{sol} is the solar flux at r_h, L_{H_2O} is the latent heat of sublimation of water ice, and A is the geometrical albedo taken equal to 0.04. In the isothermal case (model 1 in Table 2), $Z_{H_2O} = F_{sol}(1 - A)/4fL_{H_2O}$, where $f = (1 + \kappa^{-1})^{-1}$ is the icy area fraction. These equations assume a fast rotator. For computing the nucleus radius R_n, we set $4\pi R_n^2 = S_{icy}/f$.
24. We modeled the temporal evolution of the total outgassing rate of a population of icy debris, taking into account their decrease in size with time t due to sublimation according to $a(t) = a(0)(1 - t/\tau_d)$. Initial conditions are the size distribution $a^{-\alpha}$, with $a_{min} < a < a_{max}$, and the total mass at $t = 0$. The decrease of the HCN production rate observed after 23.9 July can be fitted by indexes other than $\alpha = 3.5$ but always requires that the maximum size of the debris is less than a few decimeters. Because the time sampling of our observations, the fit is not sensitive to icy grains with lifetimes smaller than one day ($a <$ 7 cm).
25. J. K. Harmon, D. B. Campbell, S. J. Ostro, M. C. Nolan, *Planet. Space Science* **47**, 1409 (1999).
26. N. Biver, thesis, Université de Paris VII (1997).
27. D. Bockelée-Morvan, T. Y. Brooke, J. Crovisier, *Icarus* **116**, 18 (1995).
28. B. G. Marsden, *IAU Circ. 6521* (1996).
29. M. Fulle, H. Mikuz, M. Nonino, S. Bosio, *Icarus* **134**, 235 (1998).
30. Compiled from the International Comet Quarterly (ICQ).

31. We thank J. Bauer and S. Sheppard for their help during the CSO observations, B. Marsden and D. Green for providing ephemerides, and J.-F. Crifo for fruitful discussions. N. Biver was supported partly by a JCMT fellowship at the University of Hawaii. This work was supported by the Programme National de Planétologie de l'Institut National des Sciences de l'Univers (INSU) and the Centre National de la Recherche Scientifique (CNRS). The JCMT is operated by the Joint Astronomy Centre on behalf of the Particle Physics and Astronomy Research Council of the United Kingdom, the Netherlands Organisation for Scientific Research, and the National Research Council of Canada. The Nançay Radio Observatory is operated by the Unité Scientifique de Nançay of the Observatoire de Paris, associated with the CNRS and also gratefully acknowledges the financial support of the Conseil Régional de la Région Centre in France. The National Radio Astronomy Observatory (NRAO) is operated by Associated Universities, under contract with the NSF. The CSO is supported by the NSF.

21 December 2000; accepted 12 March 2001

Charge Exchange–Induced X-Ray Emission from Comet C/1999 S4 (LINEAR)

C. M. Lisse,[1]* D. J. Christian,[1,2] K. Dennerl,[3] K. J. Meech,[4] R. Petre,[5] H. A. Weaver,[6] S. J. Wolk[7]

Using soft x-ray observations of the bright new comet C/1999 S4 (LINEAR) with the Chandra x-ray observatory, we have detected x-ray line emission created by charge exchange between highly ionized solar wind minor ions and neutral gases in the comet's coma. The emission morphology was symmetrically crescent shaped and extended out to 300,000 kilometers from the nucleus. The emission spectrum contains 6 lines at 320, 400, 490, 560, 600, and 670 electron volts, attributable to electron capture and radiative deexcitation by the solar wind species C^{+5}, C^{+6}, N^{+7}, O^{+7}, and O^{+8}. A contemporaneous 7-day soft x-ray light curve obtained using the Extreme Ultraviolet Explorer demonstrates a large increase in the comet's emission coincident with a strong solar flare on 14 and 15 July 2000.

Fifteen comets have now been detected in x-rays, using the BeppoSAX, Extreme Ultraviolet Explorer (EUVE), and Röntgen Satellite (ROSAT) spacecraft (*1–7*). Comparison of these results shows that (i) the emission is confined to the cometary coma between the nucleus and the Sun in a region 10^5 to 10^6 km in extent; (ii) that it is not correlated with extended dust or plasma tails; (iii) that it is not correlated in time with the solar x-ray flux; (iv) that the spectrum is soft with little C (0.28 keV) or O (0.53 keV) K-shell line emission; (v) that it is not due to scattering or resonance fluorescence or dust-dust impacts; and (vi) that all comets within 2 AU of the Sun and brighter than $\mathbf{V} = 12$ were detected. The emission scales roughly as $Q_{gas}^{0.50}$, where Q_{gas} is the gas production rate from the comet, and decreases at high levels of cometary dust production, Q_{dust}. Current models (e.g., model thermal bremsstrahlung continuum with kT $\sim$ 0.25 keV) predict a spectrum strongly increasing in intensity with increasing wavelength in the extreme ultraviolet (EUV)/soft x-ray region of the spectrum, with emission due to resonance fluorescence of solar x-rays contributing at most 20% from lines of atomic O at 530 eV and atomic C at 280 eV (*3, 4*).

Numerous potential physical mechanisms responsible for the emission have been pub-